



Evaluation of Dynamic Pressure-Sensitive Paint for Improved Analysis of Cavity Flows and CFD Validation

David A. Roberts¹ and Neil P. Stokes²
Aircraft Research Association, Bedford, United Kingdom, MK41 7PF.

Mark K. Quinn³
The University of Manchester, Manchester, United Kingdom, M1 3NJ

Joe H. Coppin⁴ and Trevor J. Birch⁵
Defence Science and Technology Laboratory, Fareham, United Kingdom, PO17 6AD

This study has investigated the use of Dynamic Pressure-Sensitive Paint (DPSP) to analyse the complex multi-dimensional flow-field within a generic small-scale rectangular planform cavity. The analysis and understanding of cavity flows have received renewed interest due to the low-observability requirements for modern military aircraft and Unmanned Combat Aerial Vehicles (UCAVs). This study has demonstrated the use of DPSP to provide unsteady pressure data, from the full model surface coverage of a model-scale cavity ceiling in a transonic Mach number range of $0.70 \leq M \leq 0.95$. These results were compared against traditional point transducer measurements and also compared with numerical simulations of the cavity flow-field. These comparisons demonstrate that DPSP represents a very useful tool for the validation of numerical data as well as for flow-diagnostic investigations, where point measurements from transducers would provide spatially limited data. Further analysis of the transducer and DPSP data has also demonstrated temporal intermittency of the widely known Rossiter modes within the cavity acoustic signature. This instability has been previously linked to mode switching and a breakdown in the modal generation feedback process within the cavity flowfield.

¹ Technical Team Leader, Aerodynamic Capabilities Business Unit, Aircraft Research Association, Manton Lane, Bedford, United Kingdom, MK41 7PF.

² Optical Measurement Systems Manager, Experimental Aerodynamics Department, Aircraft Research Association, Manton Lane, Bedford, United Kingdom, MK41 7PF.

³ Lecturer, School of Mechanical, Aerospace and Civil Engineering, The University of Manchester, George Begg Building, Sackville Street, Manchester, M1 3NJ.

⁴ Aerodynamicist, Platform Systems Division, DSTL, Fareham, United Kingdom, PO17PO12 6 AD

⁵ Aerodynamics Fellow, Platform Systems Division, DSTL, Fareham, United Kingdom, PO17PO12 6 AD, Senior Member AIAA.

Nomenclature

CFL	= Courant–Friedrichs–Lewy number	t_s	= Sample length (s)
DPSP	= Dynamic Pressure-Sensitive Paint	T_0	= Total temperature (K)
f	= Frequency (Hz)	U_∞	= Freestream velocity (ms^{-1})
f_s	= Sampling Frequency (Hz)	w	= Cavity width (m)
h	= Cavity depth (m)	x	= Cavity length ordinate (m)
k	= Rossiter vortex convection constant	y	= Cavity width ordinate (m)
l	= Cavity length (m)	α	= Rossiter phase lag constant
M	= Mach number	δf	= Frequency resolution (Hz)
m	= Rossiter mode number	δt	= Temporal resolution (s)
St	= Strouhal number	ε	= Wall porosity (%)
STFT	= Short-Term Fourier Transform	λ	= Wavelength (m)
t	= Time (s)		

I. Introduction

Cavity flows have been the subject of aerodynamic research since the early days of high-speed aircraft with internal store carriage in the 1950s^{1,2}. Low observability design requirements for current combat aircraft has renewed the interest in this field. The presence of an open cavity, such as a weapon or undercarriage bay, exposed to a high-speed grazing flow can result in severe pressure fluctuations. These pressure fluctuations can reach intensities of up to 165dB SPL and may cause damage to both the aircraft and to any sensitive components within the bay^{1,2}. Results for this study were generated using an existing generic rectangular planform cavity wind tunnel model, designated as M219/1. This small scale model was the forerunner for the more widely known larger scale M219 generic cavity model.

This study aims to investigate the unsteady pressure fluctuations over the entire cavity ceiling using: unsteady pressure transducers; Dynamic Pressure-Sensitive Paint (DPSP); and numerical simulations. DPSP has the benefit of full surface coverage allowing for a surface map of the unsteady pressures to be generated, similar to what numerical approaches can provide. This surface coverage would otherwise be prohibitively complex and expensive to achieve using unsteady transducers alone. DPSP analysis of cavity flows has so far received little attention³ and is clearly a promising investigation technique for future developments.

The data from DPSP can also be used to validate unsteady numerical simulations in a way standard transducer data cannot. This study compares data obtained from both DPSP and numerical simulations to assess the suitability of both techniques for the measurement of unsteady cavity pressures. Short-Term Fourier Transforms (STFT) of the DPSP data will be used to investigate how the modal characteristics vary both temporally and spatially over the cavity ceiling.

A. Cavity flow background

The flow characteristics within cavities exposed to high-speed grazing flows can be broadly categorised into two states referred to as “open” and “closed” flows². For an open flow state the boundary layer approaching the front wall of the cavity detaches and forms a shear layer which spans the entire cavity length. This shear layer reattaches at, or downstream, of the cavity rear wall, so that vortices constrained within the shear layer are convected downstream and impinge at the rear wall stagnation point. This impingement results in the upstream propagation of the pressure waves within the cavity and these two actions, vortex impingement and pressure wave propagation, form a feedback loop. For closed flows, the shear layer from the front wall of the cavity reattaches at some point on the cavity ceiling and therefore breaks the feedback loop. Therefore for closed flows, the undesirable large amplitude pressure fluctuations are generally not observed. However, closed flow cavities can exhibit a strong adverse pressure gradient which can affect store separation characteristics by creating an undesirable nose up pitching moment. Typically, open flow cavities have an aspect ratio (l/h) $l/h < 6$, whereas closed flow cavities have $l/h > 10$. A transitional region also exists between the two states which depends on the Mach number of the freestream flow².

Open flow cavities exhibit strong modal characteristics, which are supported by the previously described feedback mechanism. The frequencies at which these modal peaks in pressure amplitude occur can be estimated

using the modified Rossiter equation (Eq. 1), where α is typically regarded as the phase delay between the impingement of the vortices at the rear wall and the propagation of the pressure waves within the cavity and k is the ratio of the vortex convection speed to the freestream velocity (U_∞), where the value of k is often taken to be $k=0.57$ ². The non-dimensional Strouhal number (St) is used to remove the influence of model scale and freestream velocity on the frequencies of the modes, known as Rossiter modes or tones.

$$St = \frac{fl}{U_\infty} = \frac{m - \alpha}{M_\infty \left(1 + \frac{\gamma - 1}{2} M_\infty^2 \right)^{\frac{1}{2}} + \frac{1}{k}} \quad (1)$$

II. Description of experimental setup

A. The ARA Z4 transonic wind tunnel and generic cavity model

The ARA Z4 tunnel is nominally a 1/12th scale version of the ARA Transonic Wind Tunnel and comprises a 228.6mm x 203.2mm (9" x 8") working section. The tunnel is operated by means of high-pressure air ejectors located downstream of the working section and the tunnel has a nominal Mach number range of between $0.2 < M < 1.3$, where the supersonic Mach numbers are achieved through the use of a flexible nozzle upstream of the working section. Within the working section the upper and lower surfaces are both perforated with an approximate porosity (ϵ) of $\epsilon=18\%$ and diverge at an angle of approximately 0.1° . For the current work the cavity model was installed into the starboard wall of the tunnel (Fig. 1). To provide optical access for the Dynamic Pressure Sensitive Paint (DPSP) a second solid wall with an optical window was installed on the port wall. Therefore, the two sidewalls of the tunnel were solid for this test.

The model is a generic rectangular planform cavity with a length of $l=254\text{mm}$ and a width of $w=63.5\text{mm}$. The aspect ratio of the cavity (l/h) could be varied through setting the ceiling at different depths (h). For this test the unsteady flowfield for three different l/h ratios was investigated where the datum case was for $h=38\text{mm}$ depth. Details of the cavity dimensions and the expected cavity flow state are provided in Table 1.

ID	l (mm)	h (mm)	w (mm)	l/h	Expected flow state
Deep	254.0	19.1	63.5	13.3	Open
Datum	254.0	38.1	63.5	6.7	Open
Shallow	254.0	76.2	63.5	3.3	Closed

Table 1. Details of the cavity model dimensions and the expected cavity flow state

To impose a representative boundary layer thickness to cavity depth ratio (δ/h) the cavity model was installed with a splitter plate arrangement to remove the tunnel boundary layer (discussed later with Fig. 4a showing the numerical arrangement). The sharp leading edge of the plate was 150mm ahead of the cavity front wall with a transition band, formed from approximately 0.1mm diameter ballotini, located 8mm downstream of the leading edge. The boundary layer over the cavity was not measured during this entry, however, it was estimated using a flat plate approximation for turbulent boundary layers to have a relative thickness of $\delta/h=8.2\%$ for the datum cavity build ($h=38\text{mm}$) at Mach 0.90. The Reynolds number based on the cavity length was estimated to be 2.1×10^6 for Mach 0.90 flow. Throughout the test, data was gathered at Mach numbers of 0.70, 0.80, 0.85, 0.90, and 0.95.

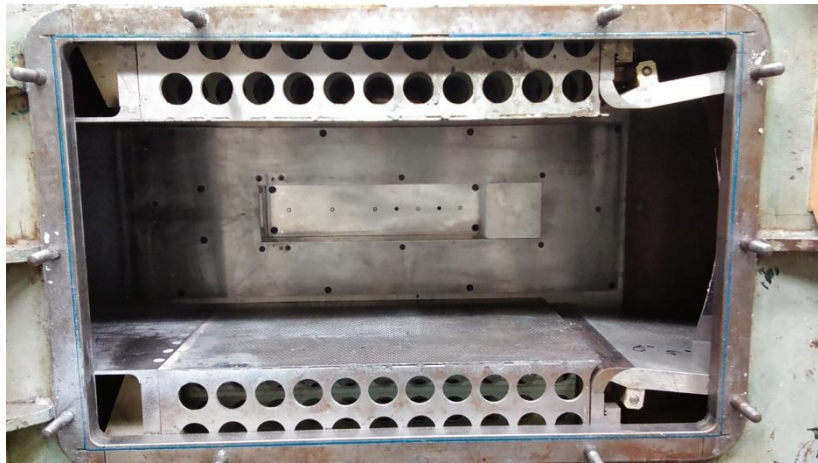


Figure 1. The generic cavity model installed into the ARA Z4 transonic wind tunnel.

B. Transducer data acquisition and analysis

The cavity ceiling was instrumented along its centreline with 5 unsteady pressure transducers (Kulite XCS-190M-15A) at fractional cavity lengths (x/l) of 0.1, 0.3, 0.5, 0.7, and 0.9 (Fig. 2). The tunnel static pressure (P) was measured from a static pressure tapping located on the tunnel floor at a location corresponding to a cavity fractional length of $x/l=0.1$. The tunnel total pressure (P_0) was measured using a Pitot probe located upstream within the settling chamber of the tunnel and it was assumed that there would be no loss in total pressure between the measurement location and working section. Both tunnel pressures (P and P_0) were measured using Druck 15psi differential transducers.

All pressure transducer signals were amplified by a gain of 20 using a Fylde FE-579-TA and filtered at 50kHz using a Fylde FE-301-SF filter to avoid aliasing in the frequency domain. The pressure transducers were sampled at a rate of $f_s=80\text{kHz}$ for a sample period of $t_s=5\text{s}$ using a National Instruments DAQ NI USB 6259. The transducers used to measure P and P_0 , and therefore calculate Mach number, were not high-bandwidth devices. Therefore, the Mach number for each sample period was calculated from the time-average of the P and P_0 measurement. To analyse the unsteady pressure measurements from the cavity ceiling the data were split into 47 blocks of length 2^{13} samples with each block having a 50% overlap. Each block was then windowed using the Hanning function and analysed using a fast Fourier transform. An ensemble average of the 47 blocks was then calculated to produce the final spectral data with a frequency resolution of 9.8Hz.

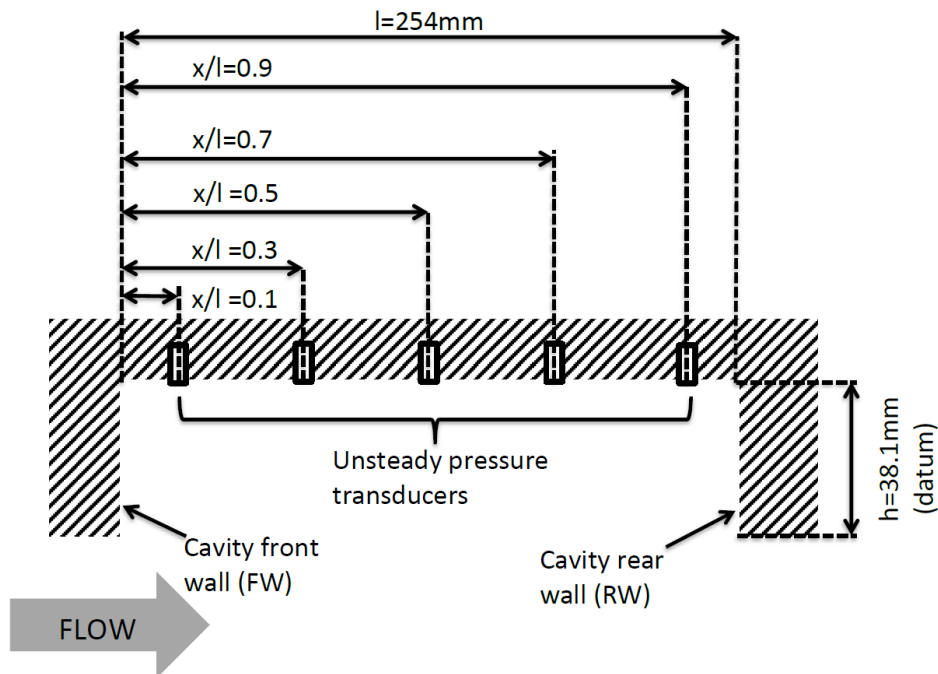


Figure 2. Unsteady pressure transducer locations on the cavity ceiling.

C. Dynamic pressure-sensitive paint acquisition and analysis

Dynamic Pressure-Sensitive Paint (DPSP) was used to investigate the spatial variations in the unsteady pressure over the cavity ceiling. Pressure-sensitive paints are sensitive to the local partial pressure of oxygen through a process called oxygen quenching. When a luminescent molecule absorbs a photon of the correct wavelength, the molecule transitions to an excited energy state. The molecule then has to recover to the standard ground state through the emission of a photon at longer wavelength compared to the absorbed photon. The rate at which this process occurs is proportional to the local partial pressure of oxygen, therefore the output intensity of the paint molecule is related to the static pressure over its surface. To account for inconsistencies in illumination and paint surface finish over the model the pressure is calibrated against the quotient of the wind-on and a wind-off reference image, where the model is at a consistent known pressure⁴.

Typically, the luminescent molecule, known as a luminophore, is incorporated into an oxygen-permeable binder material to allow the coating to adhere to a model surface. This standard formulation has the disadvantage of slow response to changes in pressure due to the finite time for oxygen diffusion through the paint coating. To achieve a faster response to changes in pressure, the luminophore molecule is sprayed onto a porous binder layer. The porosity of this layer allows for oxygen to quickly diffuse into the paint layer enabling a faster response from the oxygen quenching process.

For this test ISSI Porous Fast-Response Pressure-Sensitive Paint⁵ was used and this was illuminated by two ISSI LM2XX-DM 2inch water cooled LED lamps. These lamps provided a constant illumination output with a wavelength (λ) of $\lambda=4\times 10^{-4}\text{m}$. Images of the cavity ceiling were recorded at a sample rate of $f_s=10\text{kHz}$ using a Vision Research Phantom V1610 high-speed camera, which provided images with a bit depth of 2^{12} . The 10kHz sample rate was used because this is the highest possible sample rate possible for the illumination whilst maintaining the maximum resolution at 1280x800 pixels. The camera and the lamps were mounted externally to the Z4 tunnel to provide constant illumination over the entire cavity ceiling (Fig. 3).

To analyse the unsteady pressures from the DPSP paint response time-history required a significant amount of post-processing. DPSP is a purely radiometric technique where wind-on images are referenced to an image of known condition (i.e. wind-off). To generate the wind-off reference 500 frames were averaged. To reduce noise within the image a 3x3pixel Gaussian filter was applied to each frame of data captured including the wind-off reference. No alignment was required due to the camera being mounted externally to the tunnel and there being no model attitude changes between the reference and wind-on conditions. A calibration was performed between the intensity response of the paint and the time-averaged static pressure from the transducers. To process the DPSP data into the frequency domain, a blocklength of 128 samples with an overlap of 70% were used with Welch's PSD method. This produced DPSP data with a frequency resolution of approximately $\delta f=78\text{Hz}$ which is more than sufficient to determine the characteristics of the modal frequencies.



Figure 3. Setup of high-speed camera and constant illumination LED light sources mounted externally to the Z4 tunnel.

D. Description of testing

Overall the unsteady pressure characteristics of three different cavity configurations were investigated using both DPSP and unsteady pressure transducers over the Mach number range $0.70 \leq M \leq 0.95$ as detailed in Table 2. For each of these runs the acquisition of both the transducer and DPSP data was triggered simultaneously, but due to the different sample rates used for each technique the data cannot be considered to be simultaneous, but can be considered to be concurrent. Therefore, no phase or time-delay relationships can be calculated between the transducer and Dynamic Pressure-Sensitive Paint data sets.

Case	h (mm)	l/h	Mach numbers
Datum	38	6.7	0.70, 0.80, 0.85, 0.90, 0.95
Datum (repeat)	38	6.7	0.70, 0.80, 0.85, 0.90, 0.95
Deep	80	3.2	0.70, 0.80, 0.85, 0.90, 0.95
Shallow	19	13.4	0.70, 0.80, 0.85, 0.90, 0.95

Table 2. Table of test conditions and model configurations

III. Description of numerical simulations

Numerical simulations were performed for two geometries, the 38mm and 80mm deep cavities, at a freestream Mach number of 0.80. In order to capture the unsteady flow behaviour in the cavity, a time accurate detached eddy simulation (DES) model was run which uses Reynolds averaged Navier-Stokes (RANS) near to the wall to reduce computational cost and a large eddy simulation (LES) model in the separated flow region far from the walls.

A. Geometry and mesh description

The geometry modelled in the numerical simulations is shown in Fig. 4a. The splitter plate and plinth geometry were included in the calculations as the boundaries of the plate are close to the cavity edges – this is often excluded from this type of calculation. The wind tunnel walls were not included in the model because there was no affordable way to model the perforated walls in the CFD code. The effect of the walls is not known. The rectangular far-field boundary extends 6 meters ($23l$) up and downstream of the cavity and 5 meters ($19l$) on each side.

Unstructured, hex-dominant and prism layer meshes were generated for both cases using the BoxerMesh software. The mesh for the 38mm cavity is shown in Fig. 4b. Inside the cavity the mesh is isotropic with a spacing of $\Delta x=1\text{mm}$ giving $l/\Delta x=254$. This results in mesh sizes of 12 and 14 million cells for the two geometries.

Adiabatic wall boundary conditions were applied to all solid surfaces and a Riemann far-field boundary condition was used to represent the freestream flow at the wind tunnel conditions.

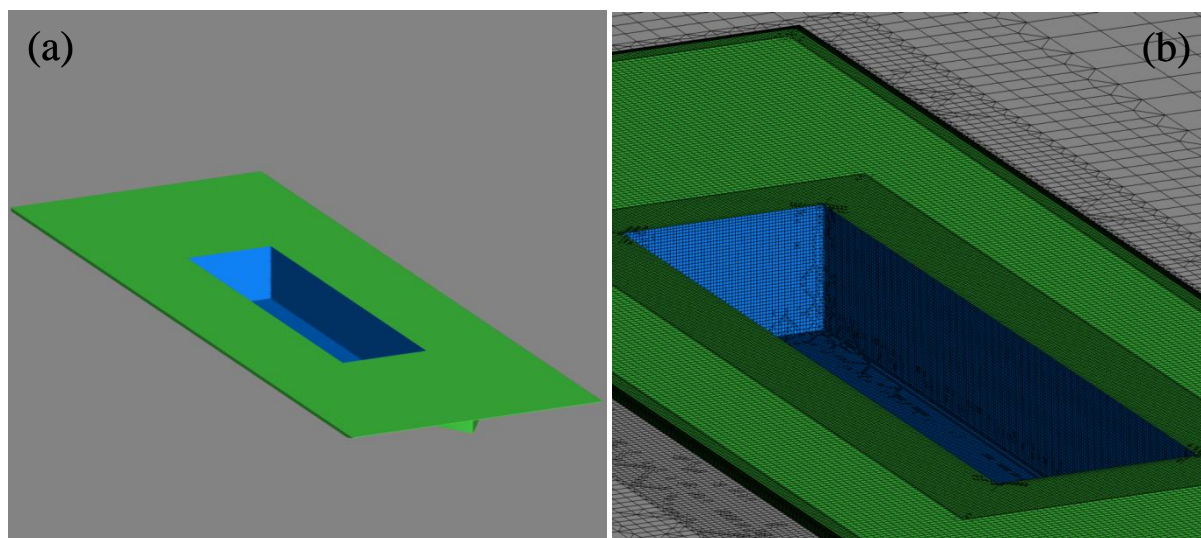


Figure 4. CFD geometry (a) and mesh (b)

B. Flow solver and processing

Calculations were carried out using Cobalt⁶ v6.1, a general purpose, unstructured, Navier-Stokes flow solver. The delayed detached-eddy simulation model⁷ was used with the Spalart-Allmaras turbulence model to predict the effects of fine-scale turbulence.

The solver was run with 2nd order discretisation in space and in time and two Newton sub-iterations per time-step were run. This model has previously been used to obtain excellent agreement with experiments for cavity flows on an aircraft configuration⁸.

A time-step of $\Delta t = 3 \times 10^{-6}$ s was used in order to give a *CFL* number of approximately 1 in the isotropic cells in the cavity. The solver was initially run for 5000 time steps to allow the flow to establish itself and to flush out any transients and then data was recorded for 100,000 time steps giving a sample length of 0.3s. Data was recorded every 8 steps giving 12500 samples. Data was sampled at the transducer locations and in a grid of 75x300 points on the cavity ceiling to compare with the DPSP results.

The data was processed using a Fast-Fourier Transform method, which was then scaled accordingly to Power-Spectral Density (PSD). The process was conducted with a sample size of 2048 and a 50% overlap, which, allows an ensemble average of 11 data blocks and gives a frequency resolution of approximately $\delta f = 20$ Hz.

Case	Mesh	Turb Model	Mach	p_{inf} (Pa)	T_{inf} (K)	Δt
1	38mm	DES-SA	0.8	65696.7	244.4	3×10^{-6}
2	80mm	DES-SA	0.8	65696.7	244.4	3×10^{-6}

Table 3: CFD Cases Run

C. Flowfield observations from the numerical results

Flowfield visualisation of the instantaneous numerical results (Fig. 5a and 5b) reveals that the flow at the leading edge of the cavity rig may not be attached or steady as was probably the intention with the design of this rig. The wedge shaped leading edge of the splitter plate causes the flow to separate on the upper surface, reattaching some distance downstream. The presence of this separation means the boundary layer approaching the cavity cannot be predicted using approximation formulae for boundary layer thickness and is probably much thicker than anticipated. The separation is also unsteady and causes vortex shedding that flows over the cavity. This can be seen in the *q*-criterion plot (Fig. 5b) and in the centreline slices in Fig. 6. Despite these unexpected features, the setup should match what was tested in the wind tunnel and therefore the agreement should be much better than for a flat plate numerical model. This experience illustrates how useful prior information from numerical simulations can be for designing representative models or better understanding any spurious results from experiments.

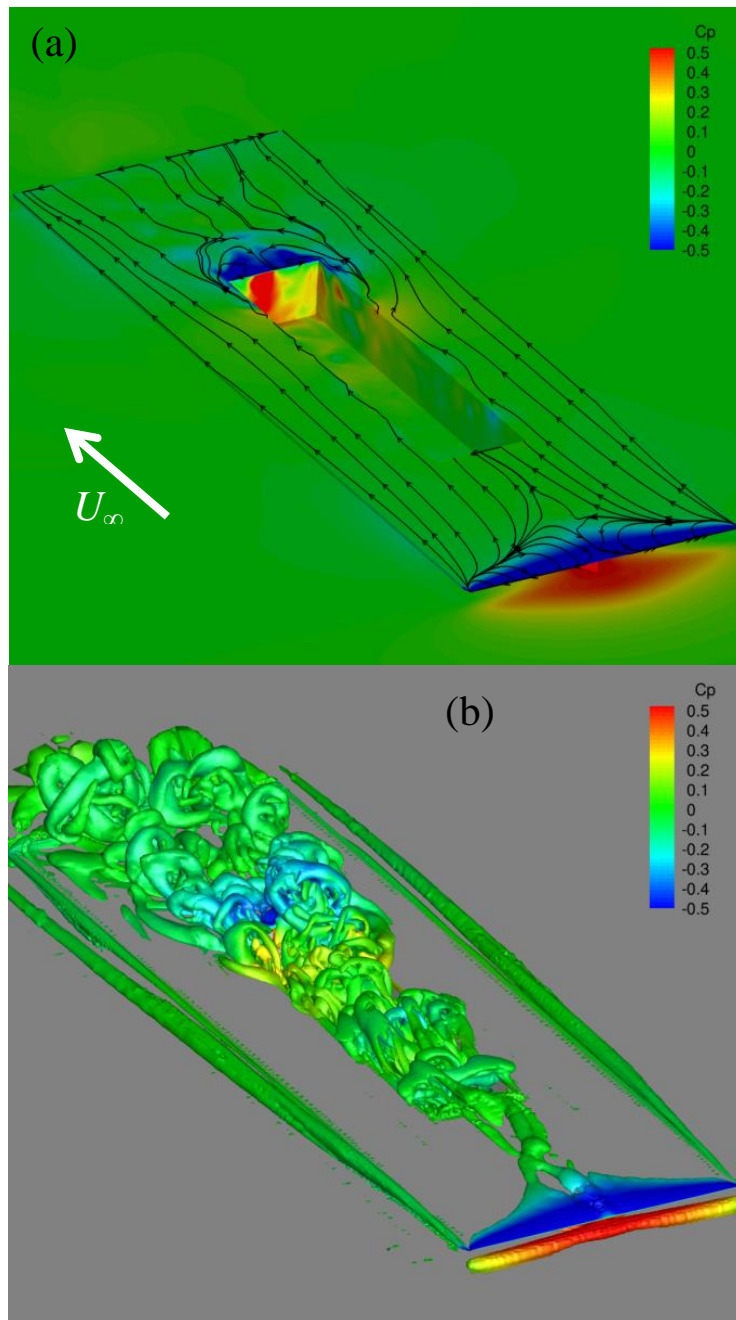


Figure 5. Surface streamlines and pressure coefficient (a) and an iso-surface of the q-criterion (b) showing flow features in and around the datum ($l/h=6.7$) cavity

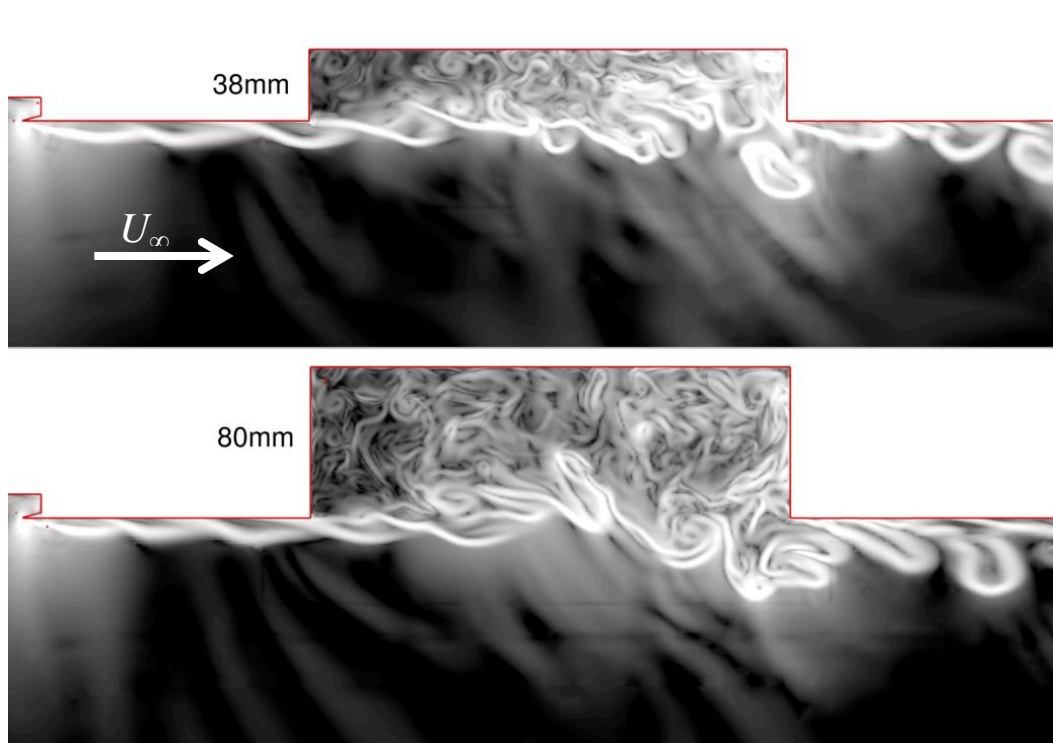


Figure 6. Contour plots along the centerline of the cavity showing the density gradient magnitude on a log scale $-\log(|\nabla\rho|)$. 38mm represents the datum cavity depth and 80mm represents the deep cavity depth.

IV. Results and discussion

This section will discuss the results from both the experimental and numerical investigations. Comparisons will be made between the two techniques to assess the potential for using DPSP to validate future numerical simulations.

A. Spectral comparisons between DPSP, transducer measurements and numerical results

Prior to the numerical investigations, the experimentally measured results were examined to provide two relevant cases for analysis, i.e. cases which exhibited strong modal behaviour. To identify the measured cavity modes the Rossiter frequencies for the first four modes were calculated using Eq. 1. These calculated frequencies are presented in Table 4 over the Mach number range $0.70 \leq M \leq 0.95$.

For the datum cavity ($l/h=6.7$) strong modal characteristics, where tonal magnitudes protruded by up to 15dB above the broadband noise levels, were exhibited at both Mach 0.80 (Fig. 7), and Mach 0.90. At Mach 0.70 and 0.95 lower tonal magnitudes were exhibited and these cases were therefore not included within the analysis of this study. For the datum cavity at Mach 0.80 (Fig. 7a and 7b) the second, third, and fourth Rossiter modes are prominent within the measured spectra at ceiling locations of $x/l=0.50$ and 0.90. As expected from previous results^{8,9,10} the measured Rossiter tonal frequencies are around 10% lower than those calculated through Eq. 1.

For all Mach numbers and locations no tone is measured at the frequency expected for the first cavity mode. However, at $x/l=0.90$ a low amplitude peak is measured at around $f_a=500\text{Hz}$ (Fig. 7b). This frequency of around 500Hz is approximately equal to the difference between adjacent tonal frequencies ($f_a=f_{n+1}-f_n$) and these difference frequencies have been previously linked to the fundamental modal generation process within cavity flows^{9,10}.

The experimentally measured transducer data and the DPSP data exhibit an excellent match for both tonal frequencies and magnitudes, where the frequencies of the two techniques are coincident and magnitudes are within 4dB. This small discrepancy between the transducer and DPSP tonal magnitude is also exhibited by the broadband noise levels from each technique. Therefore, this is most likely due to the calibration applied to the DPSP. Although the DPSP calibration is derived from the pressure transducer measurements the DPSP sensitivity is affected by temperature effects. This means any temperature gradient over the model may alter the calibration profile; also, at the reduced total temperatures at which the ARA Z4 tunnel runs ($T_0 < 283\text{K}$) the DPSP paint used is known to be less sensitive⁵. Nevertheless, this result shows that DPSP can be a powerful tool for making surface measurements with significantly increased coverage when compared with traditional transducer measurements.

The numerical results for the datum case ($l/h=6.7$) also match the measured data fairly well. Broadband noise levels are calculated to be within 1dB of the measured levels, with peak tonal magnitudes to within 4dB. The numerical results predict modal frequencies which are within 3% of those measured by the transducers (Fig. 7a and 7b). The differences between the measured and predicted sound pressure levels and numerical frequencies may be due to difficulties in modelling the flowfield over the splitter plate. Figure 5 shows that in the numerical simulation there is a significant flow separation at the leading edge of the splitter plate. However, no flowfield information is available to corroborate this from the experimentally measured dataset therefore the accuracy of these predictions is unknown.

The DPSP and transducer data exhibit better agreement for the deep ($l/h=3.2$) case, where, as with the datum case, the modal frequencies are an exact match (Fig. 8a and 8b). For the deep case the tonal amplitudes between the DPSP and transducers are measured to within 3dB and this is again attributed to the calibration process. The numerical frequency data also demonstrates better agreement with the measured data for the deep cavity case ($l/h=3.2$). For the deep cavity the frequencies calculated are again within 3% of those measured experimentally, however, the tonal intensities are within $\pm 6\text{dB}$. This again demonstrates that the DPSP technique is suitable for CFD validation.

Figure 9 shows the spectrum from a transducer located at $x/l=0.90$ on the ceiling of the shallow ($l/h=13.3$) cavity case at Mach 0.80. The spectra calculated from the data recorded by this transducer at each Mach number all demonstrate the same nominally flat profile with no tonal activity. This agrees with the expected "closed" flow state for shallow cavities. Because of this lack of tonal activity no numerical data was calculated for this case and no DPSP data is presented within this paper.

Overall, very good agreement was demonstrated between the three techniques: transducers, DPSP, and CFD. This shows that DPSP has good potential for use as a validation tool for CFD, but also is capable of providing transducer type and quality data over a greater surface coverage of a model. Unlike traditional transducer

measurements DPSP can provide unsteady pressure data over an entire surface such as the cavity ceiling demonstrated in this study.

Mode #	l/h	Calculated modal frequency (Hz)			
		Mach 0.70	Mach 0.80	Mach 0.90	Mach 0.95
1	6.7	270	292	311	320
2	6.7	730	790	842	866
3	6.7	1191	1287	1373	1412
4	6.7	1651	1785	1903	1957
1	13.3	80	86	92	95
2	13.3	540	584	623	640
3	13.3	1000	1081	1153	1186
4	13.3	1461	1579	1684	1732
1	3.3	365	395	421	433
2	3.3	825	892	952	979
3	3.3	1286	1390	1482	1524
4	3.3	1746	1888	2013	2070

Table 4. Modal frequencies calculated for the three cavity aspect ratio using Eq. 1.

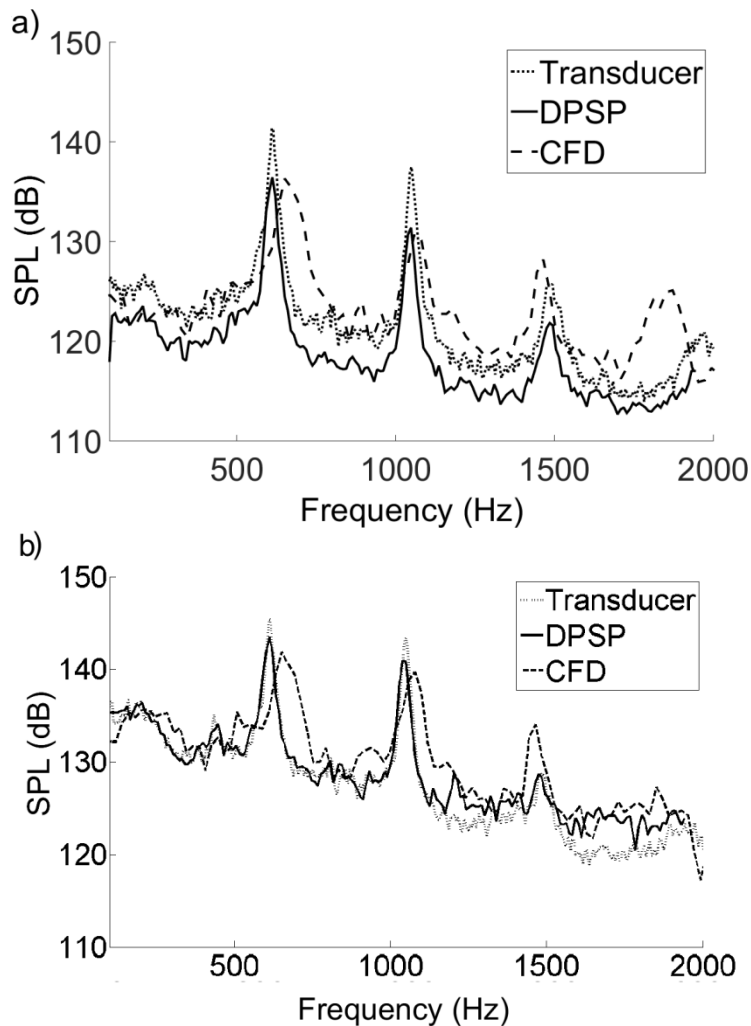


Figure 7. Comparison between spectra measured experimentally through DPSP and transducers compared with numerical results for the datum cavity ($l/h=6.7$) at Mach 0.80 for a) $x/l=0.5$, b) $x/l=0.9$

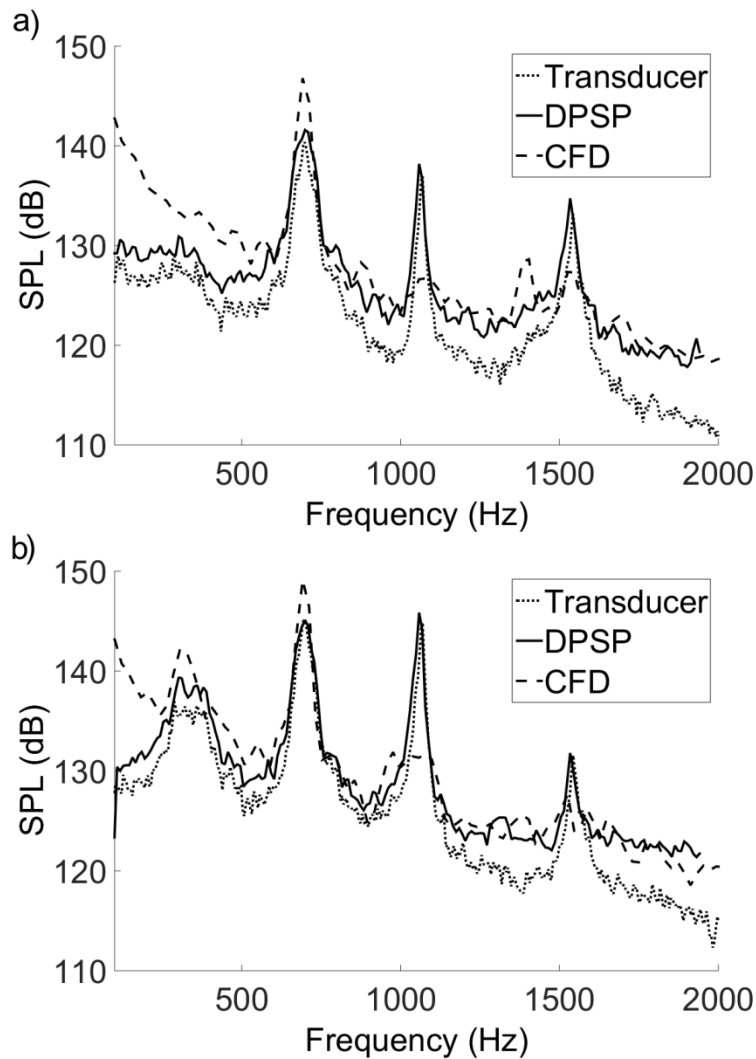


Figure 8. Comparison between spectra measured experimentally through DPSP and transducers compared with numerical results for the deep cavity ($l/h=3.2$) at Mach 0.80 for a) $x/l=0.5$, b) $x/l=0.9$

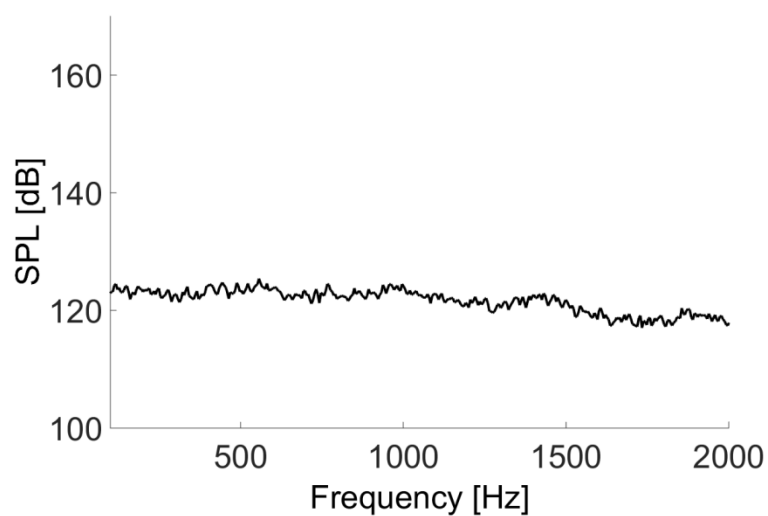


Figure 9. Spectrum measured experimentally from pressure transducers for the shallow cavity ($l/h=13.4$) at Mach 0.80 for $x/l=0.9$

B. Spatial comparisons between DPSP and numerical results

The major benefit from the DPSP technique is the spatially distributed pressure data provided. To represent the same coverage using transducers would be either prohibitively expensive or difficult to achieve due to model structural constraints. Therefore DPSP represents a very useful technique for the validation of numerical data and can generate large amounts of surface pressure data in comparably very quick timescales.

Within this section, frequency domain data, represented as Sound Pressure Levels (SPL), are presented for the datum cavity case ($l/h=6.7$) at Mach 0.80 from both DPSP and the numerical simulation. Figure 10a demonstrates that the DPSP can measure and represent the second Rossiter mode shape over the cavity ceiling. In this plot, contours of SPL clearly show the expected bi-nodal pressure distribution for the second Rossiter mode. The figure is extracted from the frequency bin containing the Rossiter tone. The two-dimensionality and location of the pressure nodes would not have been clearly defined from the transducer measurements alone, which could result in sensitive aircraft systems being located within regions of high-pressure instability.

Figure 10b shows the ceiling SPL distribution for the second Rossiter mode obtained from the numerical simulation. Again this shows the expected bi-nodal pressure distribution with SPLs approximately the same as the DPSP derived SPL values. Figure 10c shows the comparison between the DPSP and numerical SPL over the length of the cavity for a location slightly off the centreline ($y/w=0.55$) (to avoid DPSP areas of no data due to transducers). This comparison over the cavity length (Fig. 10c) demonstrates a good agreement between the measured and numerical data. Both techniques identify the locations of the pressure nodes to within $\pm 6\%$ of one another with differences in SPL over the cavity length of up to 6.5dB.

Similar agreement between DPSP and numerical data is demonstrated for the third Rossiter mode in Fig. 11 where again nodal positions agree to within $\pm 6\%$ of one another. However, for the third mode an improvement in the agreement between DPSP and numerical SPL is exhibited with levels agreeing to within 4dB (Fig. 11c).

The second mode exhibits negligible span-wise variation in SPL distribution across the ceiling (Fig. 10a and b). However, the third mode exhibits a slight tapering of the node footprint towards $y/w=0.95$. The cavity flow-field is known to be highly three-dimensional² and therefore any change in the internal flow properties would be expected to affect the formation of the modal structure.

One of the benefits of the DPSP technique is that pressure data could be gathered for more than one surface simultaneously, depending on illumination and camera view. Therefore, data could be extracted for more than one surface. For instance, this could include both the rear wall and the area on the splitter plate surrounding the cavity either side of its span. The pressure nodes formed by the Rossiter modes can be seen to extend either side of the cavity (Fig. 10a and 11a). The influence of the external flow on these structures, which are often referred to as standing wave type formations, can also be seen on the portion external to the cavity. At these positions the node is no longer orthogonal to the cavity length ordinate, where, in this instance the external flow is causing a downstream convection of the structure.

As mentioned in *section IV.A* a low-intensity peak has been identified at around 500Hz which is thought to correspond to the fundamental aero-acoustic loop frequency (f_a) within the cavity^{9,10}. However, this tone is not detectable from the initial post-processing performed on the DPSP data. This is attributed to the relatively low amplitude of the tone and the fact that it is only exhibited for the transducer located at the rear ($x/l=0.9$) of the cavity. If the DPSP technique were used within a cavity where this tone was more prominent within the acoustic signature further information could be gathered about the modal generation process and where the initial energy for the process is located within the cavity flow-field.

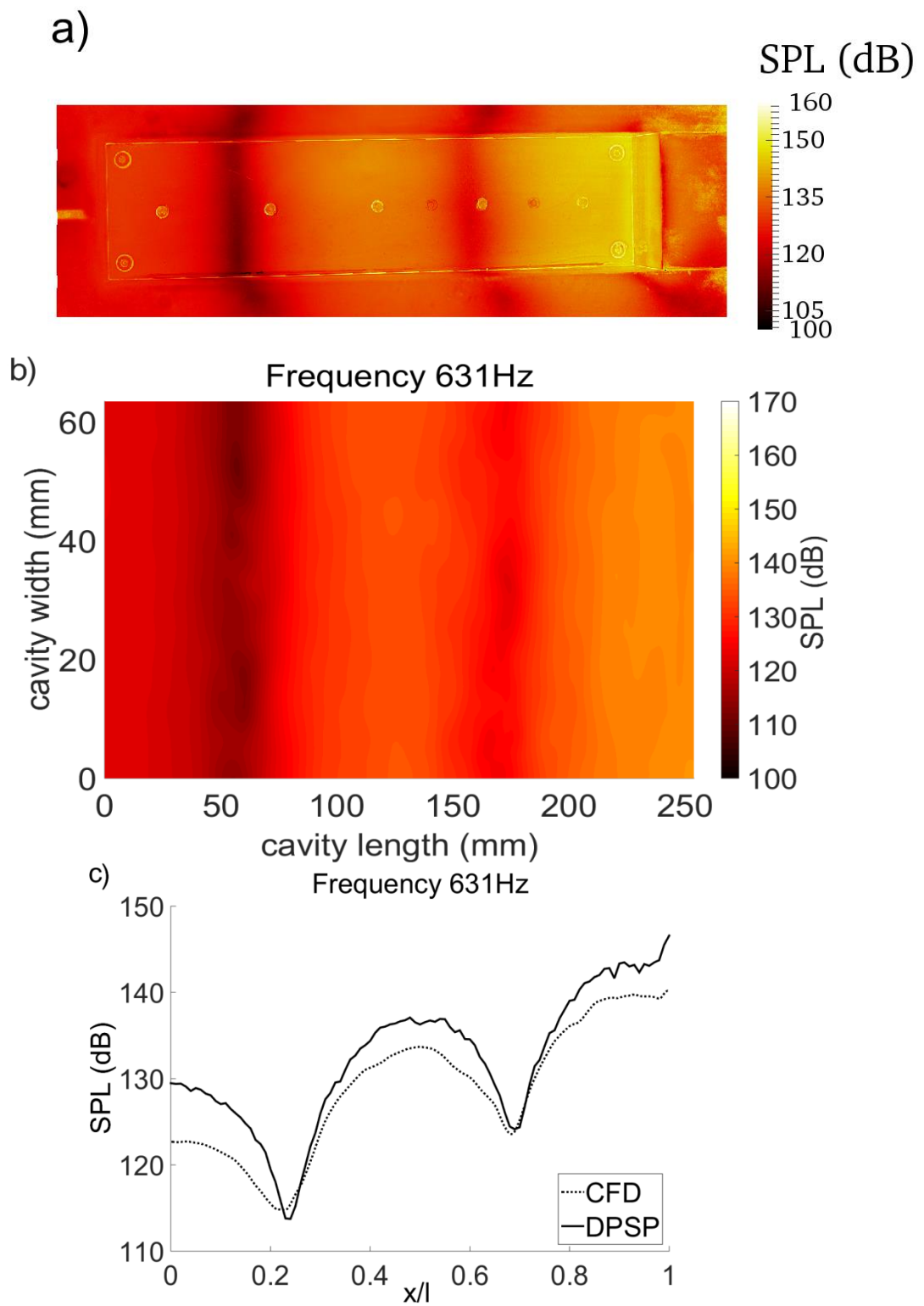


Figure 10. Contours of SPL showing the two-dimensional mode shape for the second mode (631Hz) of the datum cavity ($l/h=6.7$) at Mach 0.80 from a) DPSP measurement, b) numerical results, c) off-centreline ($y/w=0.55$) SPL distribution comparison between CFD and DPSP

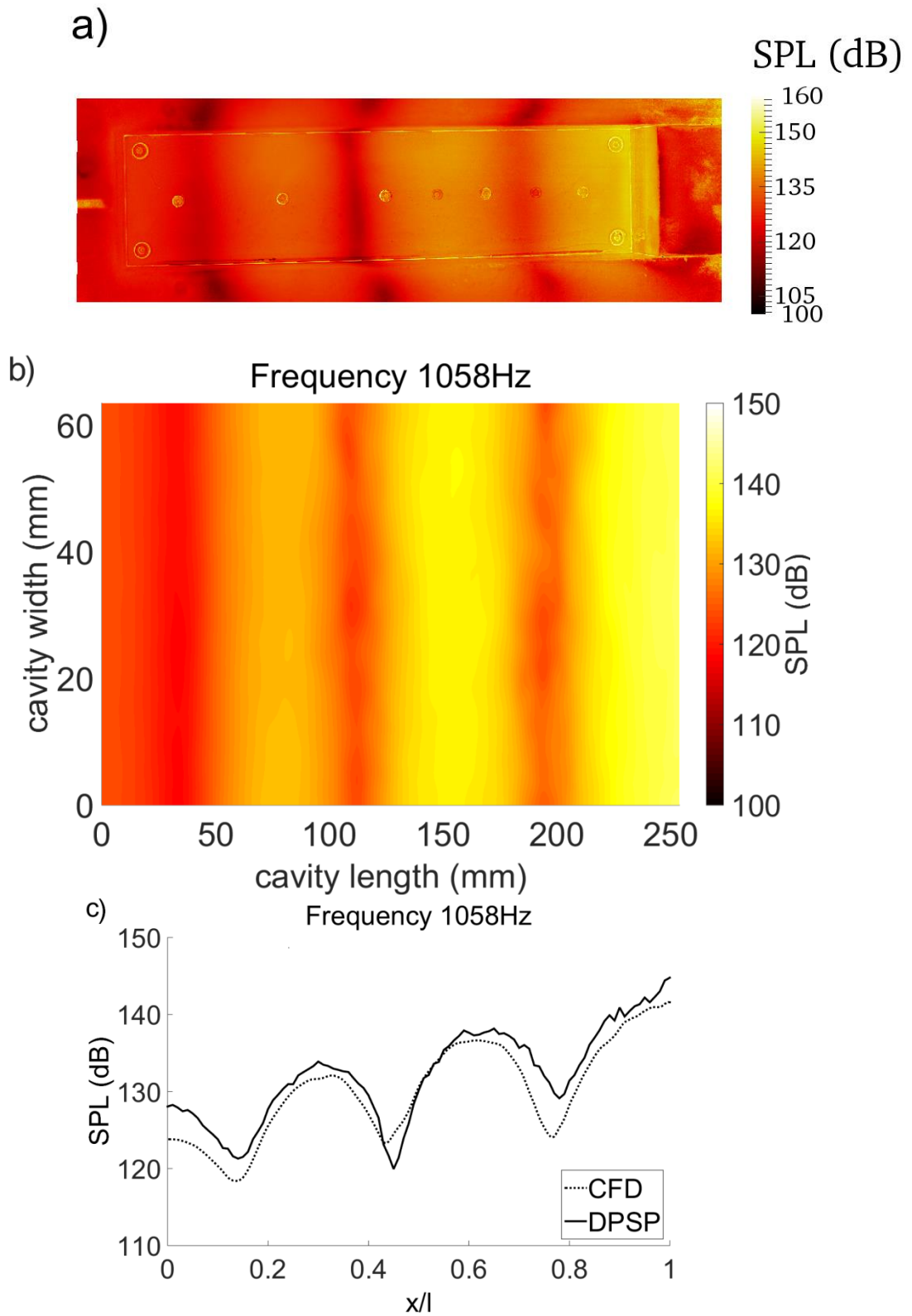


Figure 11. Contours of SPL showing the two-dimensional mode shape for the third mode (1058Hz) of the datum cavity ($l/h=6.7$) at Mach 0.80 from a) DPSP measurement, b) numerical results, c) off-centreline ($y/w=0.55$) SPL distribution comparison between CFD and DPSP

C. Short-time Fourier analysis of the cavity flow-field

Intermittency of the Rossiter modes has been previously demonstrated for “open” type cavity flow-fields at Mach numbers of: $M < 0.1$ ¹¹, $M = 0.4$ ¹², and $0.80 < M < 0.95$ ¹⁰ and has previously been referred to as “peaking”. This intermittent process involves the redistribution of energy between the cavity modes from one mode to another receptive mode. Figure 12 shows Short-Term Fourier Transform (STFT) analysis of the pressure transducer time-histories measured at $x/l=0.1, 0.5$, and 0.9 for the datum cavity ($l/h=6.7$) at Mach 0.80. This type of analysis performs frequency analysis on a series of relatively small consecutive data blocks within a time history to indicate how specific frequencies vary in time. For the STFT analysis conducted on the transducer data, a block length of 512 samples was used with a 50% overlap. This resulted in a frequency resolution of approximately $\delta f=78\text{Hz}$ and a temporal resolution of $\delta t=0.0064\text{s}$. The STFT approach necessitates a trade-off between the temporal and frequency resolution of the processed results. For this case the frequency resolution of approximately $\delta f=78\text{Hz}$ was deemed acceptable as this is around 15% of the difference between consecutive tonal frequencies (f_a) and therefore still allows for each mode to be clearly identified from the contour plots (Fig. 12). In the STFT plots the colour scales are reversed compared with the modal SPL distribution plots to clarify the time periods for the higher SPLs.

The prominent horizontal lines in each plot (Fig. 12) correspond to the Rossiter modes. Overall the tonal peaks measured by the transducers all exhibit levels of intermittency, where peak magnitudes can vary by as much as $\pm 15\text{dB}$ over short time scale (Fig. 12). Thresholding of the contour levels (Fig. 12d) further highlights the modal switching, where periods of high SPL for the second mode correspond to periods of low intensity for the third mode. As with the standard spectral plots (Fig. 7) the first mode is not well defined within the noise signature. However, previous studies¹⁰ have indicated that the intermittency of the first mode is not related to that of the second and third modes. The cause of the modal intermittency is as yet unknown, however, further insight into the modal switching process is obtained from Fig. 7, where at approximate times of 1.2s and 1.6s there appears to be a period where neither mode exhibits significant modal activity. These periods both occur before a section of third mode dominance and therefore could relate to the time required to switch energy between the different cavity modes.

Previous studies which have investigated the intermittency of the cavity modes have only used data measured from transducers and therefore only provide information about the modal characteristics for a single or range of isolated points. The advantage of the DPSP approach is that this information can be gathered across the entire cavity ceiling. Because of the limitations of the equipment the measurement of the DPSP and transducers can be described as being concurrent rather than simultaneous. Therefore, any phase or temporal correlation between the two data-sets cannot be performed. However, the STFT analysis of the transducer data does provide time periods where either the second or third cavity mode is the dominant mode within the acoustic signature. This time period can then be extracted from the DPSP time history to investigate how the modal shape and the energy at the modal frequency is distributed when the mode is switching. Overall, three time periods were examined relating to either a second or third mode dominance, where: $t=1.069\text{s}$ 2nd mode, 1.222s 3rd mode, and 1.568s 3rd mode.

For the DPSP STFT analysis, a block length of 128 samples was used with no overlap. This resulted in a frequency resolution of approximately $\delta f=78\text{Hz}$ and a temporal resolution of $\delta t=0.0128\text{s}$. Again these resolutions were deemed acceptable as they allow for both the modal structures to be determined and for switching behaviour to be demonstrated. The results of the DPSP STFT analysis are presented in Fig. 13 and Fig. 14 for the second and third modal frequencies respectively. The contour plots presented in Fig. 13 and Fig. 14 exhibit a higher level of noise (speckle) compared with those shown previously (Fig. 10 and 11), this is due to the lack of ensemble averaging during the STFT process. Each contour plot is therefore the direct output of the Welch’s PSD estimate for a single data block with the inherent signal noise associated with this processing approach.

From the DPSP data there are also clear signs of modal intermittency, where the SPL associated with the modal shape over the cavity ceiling varies in time. For the second mode (Fig. 13) the plots with a strong mode shape, i.e. well defined pressure nodes, correspond to the time expected from the transducer STFT analysis. Therefore for $t=1.069\text{s}$ (Fig. 13a) and $t=1.568\text{s}$ (Fig. 13c) the second mode exhibits a well-defined mode shape with nodal SPL around 10dB lower than in other regions. However, for $t=1.222\text{s}$ (Fig. 13b) the mode shape is less well defined and this corresponds to a period where the second mode is shown to be less dominant within the acoustic signature (Fig. 12). For this case the nodal SPL is only around 5dB lower than the surrounding regions with a much broader footprint. This indicates a weaker formation within the flowfield.

For the third mode cases again there is a relationship between when the transducer indicates a period of modal activity and when the DPSP exhibits a clear mode shape (Fig. 14). Indeed the third mode exhibits a clear modal

profile at $t=1.222$ s (Fig. 14b) when the second mode exhibits its weakest profile. As expected the modal profiles for $t=1.069$ s (Fig. 14a) and for $t=1.568$ s (Fig. 14c) are less defined and again exhibit a broadening of the nodal footprint on the cavity ceiling. This could be related to the gradual process of energy distribution between the modes.

The broadening of the nodal footprint on the cavity ceiling may be as a result of the relatively low-bandwidth output from the STFT analysis, where higher frequency oscillations of the modal structures would be under-resolved and therefore aliased within the low bandwidth output. When consecutive frames are viewed sequentially a stochastic motion of the modal footprint can be seen coupled with a periodic strengthening and weakening of the formation.

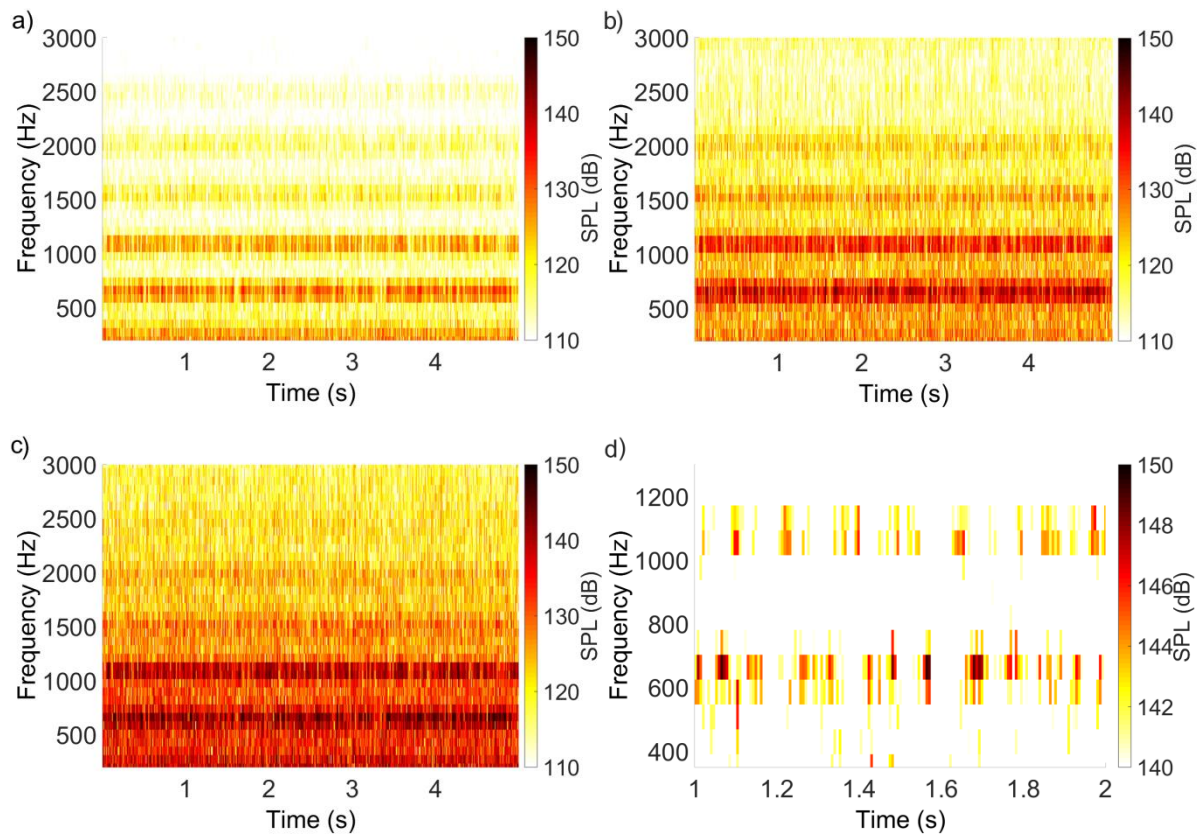


Figure 12. Short-Term Fourier analysis of the pressure measured within the datum cavity at Mach 0.80 by the transducers at a) $x/l=0.1$, b) $x/l=0.5$, c) $x/l=0.9$, d) $x/l=0.9$ with SPL threshold

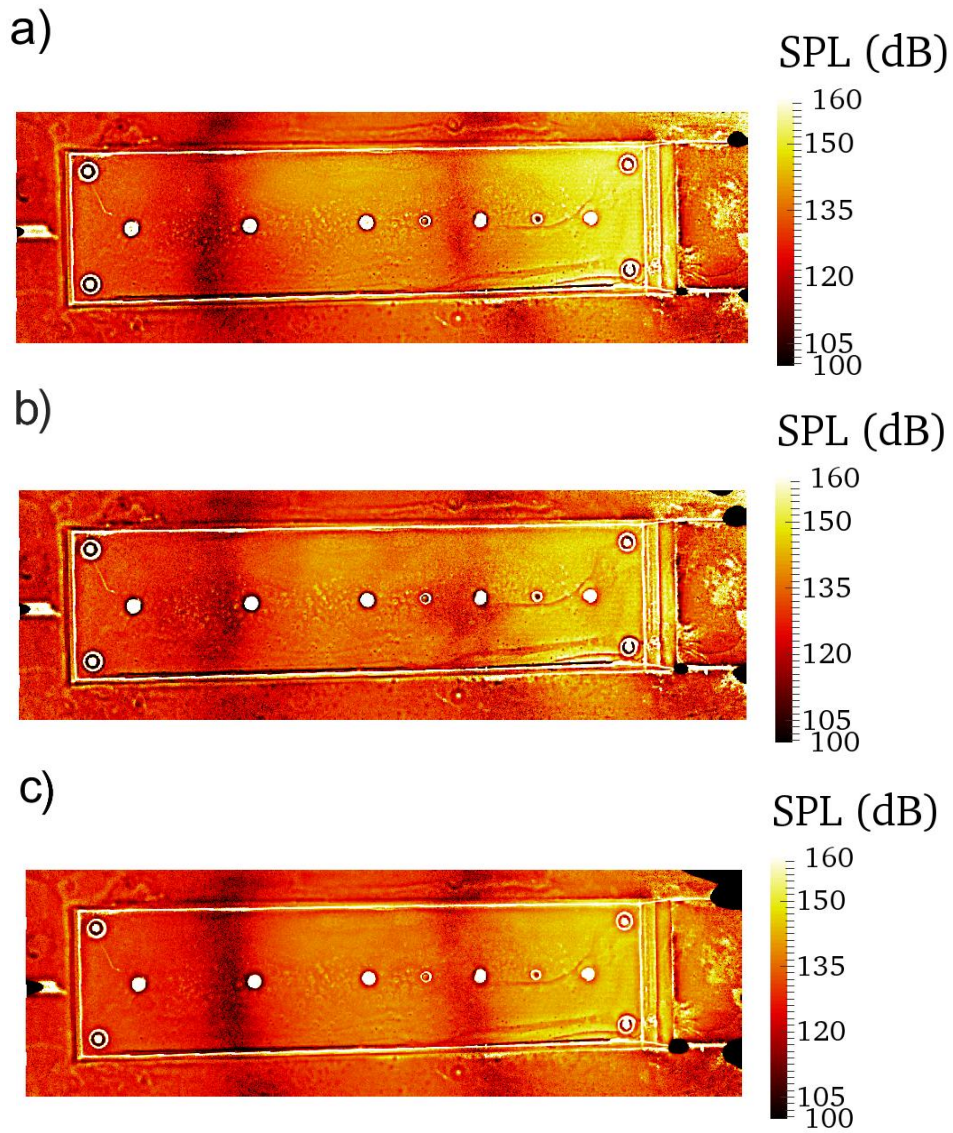


Figure 13. Short-Term Fourier analysis of DPSP data for the datum cavity at Mach 0.80. Images correspond to the second mode (631Hz) at time steps of a) 1.069s, b) 1.222s, and c) 1.568s

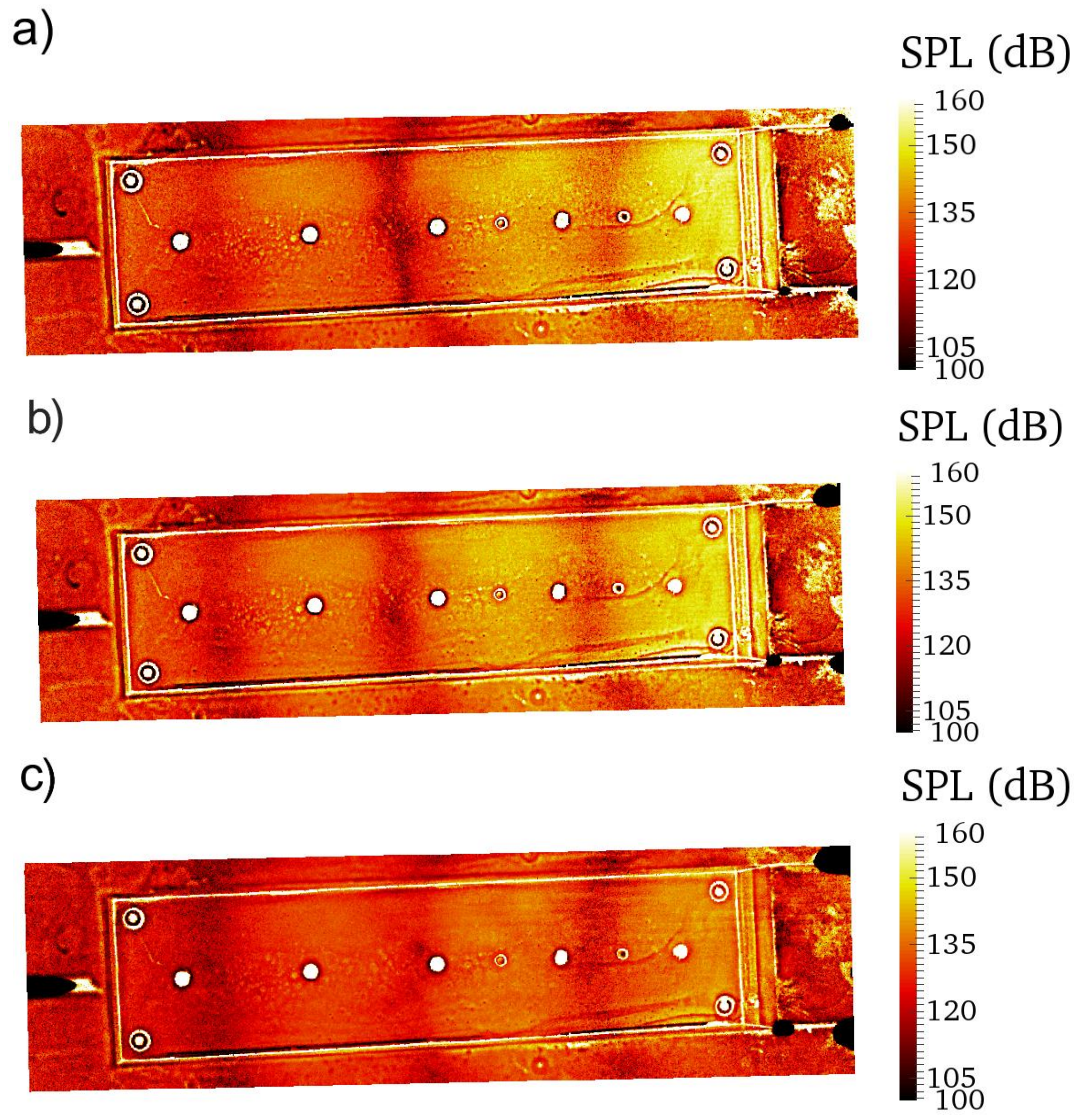


Figure 14. Short-Term Fourier analysis of DPSP data for the datum cavity at Mach 0.80. Images correspond to the third mode (1058Hz) at time steps of a) 1.069s, b) 1.222s, and c) 1.568s

V. Conclusions

An investigation of transonic cavity flow was conducted using both experimentally measured and numerically generated data sets. During the experiment unsteady pressure transducers and Dynamic Pressure-Sensitive Paint (DPSP) were used to measure the fluctuating pressure over the ceiling of a generic rectangular planform cavity. Unsteady pressures were measured at Mach numbers of $M=0.70$, 0.80 , 0.85 , 0.90 , and 0.95 for three different cavity aspect ratios: $l/h=3.2$, 6.7 , and 13.4 . In addition to these experimental cases two cases were numerically simulated at Mach 0.80 for $l/h=6.7$ and 3.2 .

The experimental and numerical data exhibited good agreement. The magnitudes of the Rossiter peaks were measured to within $\pm 3\%$ of the numerical values and the peak tonal magnitudes were measured to within $\pm 3\text{dB}$ of the numerical values for the datum ($l/h=6.7$) case. The frequency agreement improved to less than 3% for the deep cavity case ($l/h=3.2$) case, however the magnitudes were only measured to within 4dB .

Over the cavity ceiling the mode shape distribution also exhibited a very good agreement between experimental and numerical data. Mode shapes for the second and third modes show that the numerical simulation has correctly calculated the location of the pressure nodes on the cavity ceiling to within 6% of the DPSP measured values. However, the numerical data is limited by the specified output plane location and no information about the modal formations exterior to the cavity could be obtained. The DPSP demonstrated that the modal pressure nodes extend beyond either side of the cavity span. The numerical data also indicated that there could be a separation from the leading edge of the boundary layer splitter plate which is located upstream of the cavity leading edge. This separation will have affected the accuracy of the numerically generated data and may also have had an influence on the experimentally measured data if the same separation occurred during the wind tunnel tests.

The experimental data identified modal intermittency within the datum ($l/h=6.7$) cavity. This is where at an instance in time one mode appears dominant over another and energy is transferred between receptive modes. This modal switching has been identified in both the transducer and DPSP data, where the DPSP data shows the process affects how the typical Rossiter mode shapes are formed within the cavity.

Overall the DPSP method presented provides a promising approach for the study and evaluation of cavity unsteady pressures in more detail than has previously been possible with transducer measurements alone.

Further work relating to this study would include:

- To investigate the splitter plate leading edge flowfield in the experiment to see if it matches the numerical predictions where a significant separation exists. If present, could the rig be modified to eliminate this feature and provide improved (smaller δ) onset flow?
- To improve the DPSP signal-to-noise ratio for the STFT analysis through the use of overlapping blocks
- To use correlation and phase analysis of the DPSP and numerical data to further understand the modal intermittency
- Improve accuracy of DPSP predictions by implementing thermal compensation calibration

Acknowledgments

The authors would like to acknowledge Dr David MacManus from Cranfield University (UK) for his participation in the experiments and for the loan of the pressure transducers and associated data acquisition hardware.

References

- ¹ Rossiter, J., “Wind-Tunnel Experiments on the Flow over Rectangular Cavities at Subsonic and Transonic Speeds” Ministry of Aviation – Aeronautical research council, Reports and Memoranda 3438, 1966.
- ² Engineering Sciences Data Unit, “Aerodynamics and aero-acoustics of rectangular planform cavities. Part II: Unsteady flow and aero-acoustics” report 04023, 2006.
- ³ Flaherty, W., Reedy, T.M., Elliott, G.S., Austin, J.M., Schmit, R., Crafton, J., “Investigation of Cavity Flow Using Fast-Response Pressure-Sensitive Paint” *AIAA Journal*, Vol. 52, No. 11, 2014, pp. 2462-2470. DOI: 10.2514/1.J052864.
- ⁴ Gregory, J.W., Asai, K., Kameda, M., Liu, T., and Sullivan, J. P., “A review of pressure-sensitive paint for high-speed and unsteady aerodynamics” *Proceedings of the Institution of Mechanical Engineers*, Vol. 222, Part G: Journal of Aerospace Engineering, 2008, pp. 249-290. DOI:10.1243/09544100JAERO243
- ⁵ Innovative Scientific Solutions Inc., “Porous Fast-Response Pressure Sensitive Paint data sheet”, [URL :http://psp-tsp.com/PDFs/Paint%20Data%20sheets/ Porous%20Fast%20Response%20PSP%20 \(FP-XXX\)%20Data%20Sheet.pdf](http://psp-tsp.com/PDFs/Paint%20Data%20sheets/Porous%20Fast%20Response%20PSP%20(FP-XXX)%20Data%20Sheet.pdf) [cited 24 September 2015]
- ⁶ Grismer, M. J., Strang, W. Z., Tomaro, R. F., and Witzemman, F. C., “Cobalt: A Parallel, Implicit, Unstructured Euler/Navier-Stokes Solver”, *Adv. Eng. Software*, Vol. 29, No. 3-6, pp. 365-373, 1998.
- ⁷ Spalart, P. R., Deck, S., Shur, M. L., Squires, K. D., Strelets, M. K., and Travin, A., “A new version of detached-eddy simulation, resistant to ambiguous grid densities”, *Theoretical and Computational Fluid Dynamics*, 2006, pp. 181–195.
- ⁸ Chaplin, R., and Birch, T., “The aero-acoustic environment within the weapons bay of a generic UCAV”, 30th *AIAA Applied Aerodynamics Conference*, 2012.
- ⁹ Delprat, N., “Rossiter’s Formula: A Simple Spectral Model for a Complex Amplitude Modulation Process,” *Physics of Fluids*, Vol. 18, No. 7, 2006, doi:10.1063/1.2219767
- ¹⁰ Roberts, D., “Analysis and Control of Resonant Cavity Flows,” Ph.D. Thesis, School of Engineering, Cranfield Univ., Bedfordshire, England, U.K., 2013.
- ¹¹ Lusseyran, F., Pastur, L., and Letellier, C., “Dynamical analysis of an intermittency in an open cavity flow”, *Physics of Fluids*, Vol. 20, 2008.
- ¹² Kergerise, M., Spina, E., Garg, S., and Cattafesta III, L., “Mode-switching and nonlinear effects in compressible flow over a cavity”, *Physics of Fluids*, Vol. 16, No. 3, 2004.